Fabrication of Hybrid Silica Nanoparticles Densely Grafted with Thermoresponsive Poly(*N*-isopropylacrylamide) Brushes of Controlled Thickness via Surface-Initiated Atom Transfer Radical Polymerization

Tao Wu, Yanfeng Zhang, Xiaofeng Wang, and Shiyong Liu*

Department of Polymer Science and Engineering, Joint Laboratory of Polymer Thin Films and Solution, Hefei National Laboratory for Physical Sciences at the Microscale, University of Science and Technology of China, Hefei, Anhui 230026, China

Received July 28, 2007. Revised Manuscript Received October 7, 2007

This article reports on the fabrication of hybrid silica nanoparticles densely grafted with thermoresponsive poly(*N*-isopropylacrylamide) (PNIPAM) brushes and their thermal phase transition behavior. Surface-initiated atom transfer radical polymerization (ATRP) of *N*-isopropylacrylamide (NIPAM) was conducted in 2-propanol at ambient temperature using CuCl/$CuCl_2$/tris(2-(dimethylamino)ethyl)amine (Me_6TREN) as the catalytic system, starting from the surface of silica nanoparticles derivatized with ATRP initiators (0.35 nm^2/initiator). The surface-initiated ATRP can be conducted in a well-controlled manner, as revealed by the linear kinetic plot, linear evolution of number-average molecular weights (M_n) versus monomer conversions, and the relatively narrow molecular weight distributions ($M_w/M_n < 1.25$) of the grafted PNIPAM chains. The grafting density of PNIPAM chains at the surface of silica nanoparticls was estimated to be 2.2 nm^2/chain based on transmission electron microscopy (TEM) and thermogravimetric analysis (TGA) characterization results. Laser light scattering (LLS) and optical transmittance were then employed to study the thermal phase transitions of PNIPAM brushes at the surface of silica nanoparticles. Both the intensity-average hydrodynamic radius, $\langle R_h \rangle$, and average radius of gyration, $\langle R_g \rangle$, exhibit a two-stage decrease upon heating over the broad temperature range of 20–37 °C, which is in contrast to the fact that free PNIPAM homopolymer in aqueous solution exhibits a phase transition at ca. 32 °C within a narrow temperature range. The first phase transition takes place in the temperature range of 20–30 °C, which can be tentatively ascribed to the *n*-cluster-induced collapse of the inner region of PNIPAM brushes close to the silica core; the second phase transition occurs above 30 °C, which can be ascribed to the outer region of PNIPAM brushes, possessing much lower chain density compared to that of the inner part. We tentatively expect that the observed unique double phase transition behavior of polymer brushes coated at the surface of inorganic nanoparticle cores can be further utilized to fabricate novel nanostructured devices with more complex functions.

Introduction

Organic/inorganic hybrid nanoparticles have attracted ever increasing attention in the past decade due to their fascinating optical, electronic, magnetic, and catalytic properties.[1–4] Hybrid nanoparticles typically consist of polymer shells with incorporated inorganic cores. The organic polymer shell mainly determines the chemical properties of nanoparticles and their responsiveness to external stimuli, whereas the physical properties of nanoparticles are governed by both the size and shape of inorganic cores and surrounding organic layer. Hybrid nanoparticles can be prepared by either physical adsorption or covalent grafting techniques including "grafting to"[5,6] or "grafting from" methods.[7–11] Compared to the former, the latter method provides better control over the types of grafted polymer, surface grafting density, and chain lengths.

Among previously reported numerous examples of inorganic/organic hybrid nanoparticles, silica/polymer hybrid nanoparticles have been most extensively studied, probably due to their wide applications and the ease of particle synthesis. Using the "grafting from" technique, Prucker et al.[12] described the growth of polystyrene via conventional free radical polymerization from the surface of silica nanoparticles derivatized with an azo-containing monolayer. Striding progress in the field of controlled/living radical

* To whom correspondence should be addressed. E-mail: sliu@ustc.edu.cn.

(1) Caruso, F. *Adv. Mater.* **2001**, *13*, 11.
(2) Golden, J. H.; Deng, H. B.; Disalvo, F. J.; Frechet, J. M. J.; Thompson, P. M. *Science* **1995**, *268*, 1463.
(3) Daniel, M. C.; Astruc, D. *Chem. Rev.* **2004**, *104*, 293.
(4) Bourgeat-Lami, E. In *Encyclopedia of Nanoscience and Nanotechnology*; Scientific Publishers: Los Angeles, 2004; Vol. 8, p 305.
(5) Lindenblatt, G.; Schartl, W.; Pakula, T.; Schmidt, M. *Macromolecules* **2000**, *33*, 9340.
(6) Zhu, M. Q.; Wang, L. Q.; Exarhos, G. J.; Li, A. D. Q. *J. Am. Chem. Soc.* **2004**, *126*, 2656.
(7) Pyun, J.; Kowalewski, T.; Matyjaszewski, K. *Macromol. Rapid Commun.* **2003**, *24*, 1043.
(8) Mandal, T. K.; Fleming, M. S.; Walt, D. R. *Nano Lett.* **2002**, *2*, 3.
(9) Sill, K.; Emrick, T. *Chem. Mater.* **2004**, *16*, 1240.
(10) Kickelbick, G.; Holzinger, D.; Brick, C.; Trimmel, G.; Moons, E. *Chem. Mater.* **2002**, *14*, 4382.
(11) Vestal, C. R.; Zhang, Z. J. *J. Am. Chem. Soc.* **2002**, *124*, 14312.
(12) Prucker, O.; Ruhe, J. *Macromolecules* **1998**, *31*, 592.

10.1021/cm702073f CCC: $40.75
Published on Web 12/12/2007

polymerizations including atom transfer radical polymerization (ATRP), reversible addition–fragmentation chain transfer polymerization (RAFT), and nitroxide-mediated radical polymerization (NMRP) has paved the way for grafting of polymer chains with predetermined molecular weight and narrow polydispersity from the surface of silica nanoparticles.[13–36]

The surface-initiated ATRP on silica nanoparticles was first reported by Patten et al.[13,14] They successfully demonstrated that styrene (St) and methyl methacrylate (MMA) could be controllably polymerized from 75 nm silica nanoparticles. Following similar principles, a variety of other monomers such as *n*-butyl acrylate (*n*BA), *tert*-butyl acrylate (*t*BA), 2-hydroethyl methacrylate (HEMA), and oligo(ethylene glycol) methyl ether methylacrylate (OEGMA) have been polymerized from silica nanoparticles via surface-initiated ATRP.[15,16,20,24]

Recent progress in this area involves the preparation of hybrid nanoparticles coated with stimuli-responsive polymer brushes, which are attractive building blocks for the design and fabrication of smart nanostructured devices. Armes et al.[15,19] grafted pH-responsive poly(2-(diethylamino)ethyl methacrylate) (PDEA) and multiresponsive poly(2-(dimethylamino)ethyl methacrylate) (PDMA) and poly(2-(*N*-morpholino)ethyl methacrylate) (PMEMA) brushes at the surface of silica nanoparticles via ATRP. Zhao et al.[24] reported the synthesis of "hairy" silica nanoparticles grafted with mixed polymer brushes of hydrophobic PS and pH-responsive poly(acrylic acid) (PAA) via a combination of ATRP and NMRP techniques. The same research group also reported the preparation of hybrid silica nanoparticles coated with thermoresponsive poly(methoxydi(ethylene glycol) methacrylate) and poly(methoxytri(ethylene glycol) methacrylate) brushes.[26]

Perhaps the most extensively studied stimuli-responsive hybrid nanoparticles are those coated with thermoresponsive poly(*N*-isopropylacrylamide) (PNIPAM) brushes. PNIPAM has been well-known as a thermoresponsive polymer, exhibiting a lower critical solution temperature (LCST) at ~32 °C.[37] Zhu et al.[6] synthesized gold nanoparticles stabilized with thiol-terminated PNIPAM via the "grafting to" approach. Tenhu et al.[38,39] prepared PNIPAM-coated gold nanoparticles using both "grafting to" and "grafting from" approaches, and further micro-DSC studies revealed double thermal phase transitions for the PNIPAM brushes at the surface of gold nanoparticle.[40] In the above two cases, the RAFT technique was employed for the preparation of PNIPAM precursor or controlled surface grafting polymerizations.

However, surface-initiated ATRP of *N*-isopropylacrylamide (NIPAM) from nanoparticles has been rarely reported, probably due to that the ATRP of acrylamido monomers can not be well-controlled under conventional conditions.[41,42] Choi et al.[43] prepared gold nanoparticles coated with a cross-linked polymer layer via the ATRP copolymerization of NIPAM and ethylene diacrylate in water, using CuBr/2,2′-dipyridyl (bpy) as the catalyst. Just recently, Wang et al.[28] reported the synthesis of hybrid silica nanoparticles with PNIPAM shells by surface-initiated ATRP in aqueous solution, using CuCl/bpy as the catalytic system; however, the polymerization kinetics and the molecular weights and molecular weight distributions of grafted PNIPAM chains were not provided.

In the above two rare examples of surface-initiated ATRP of NIPAM from nanoparticles, water was exclusively used as polymerization solvent, which has been proved to suffer from disadvantages such as high concentration of polymeric radicals and unavoidable chain transfer or termination.[44] It has also been proved that CuX/bpy was not a suitable catalytic system for the ATRP of acrylamido monomers,[42,45] and NIPAM has not been controllably polymerized by ATRP when bpy was employed as the ligand.[46] Thus, in previous examples of surface-initiated ATRP of NIPAM from nanoparticles, the thickness of grafted PNIPAM brushes cannot be well-controlled.

(13) von Werne, T.; Patten, T. E. *J. Am. Chem. Soc.* **1999**, *121*, 7409.
(14) von Werne, T.; Patten, T. E. *J. Am. Chem. Soc.* **2001**, *123*, 7497.
(15) Perruchot, C.; Khan, M. A.; Kamitsi, A.; Armes, S. P.; von Werne, T.; Patten, T. E. *Langmuir* **2001**, *17*, 4479.
(16) Carrot, G.; Diamanti, S.; Manuszak, M.; Charleux, B.; Vairon, I. P. *J. Polym. Sci., Part A: Polym. Chem.* **2001**, *39*, 4294.
(17) Pyun, J.; Matyjaszewski, K.; Kowalewski, T.; Savin, D.; Patterson, G.; Kickelbick, G.; Huesing, N. *J. Am. Chem. Soc.* **2001**, *123*, 9445.
(18) Mori, H.; Seng, D. C.; Zhang, M. F.; Muller, A. H. E. *Langmuir* **2002**, *18*, 3682.
(19) Chen, X. Y.; Randall, D. P.; Perruchot, C.; Watts, J. F.; Patten, T. E.; von Werne, T.; Armes, S. P. *J. Colloid Interface Sci.* **2003**, *257*, 56.
(20) Pyun, J.; Jia, S. J.; Kowalewski, T.; Patterson, G. D.; Matyjaszewski, K. *Macromolecules* **2003**, *36*, 5094.
(21) El Harrak, A.; Carrot, G.; Oberdisse, J.; Eychenne-Baron, C.; Boue, F. *Macromolecules* **2004**, *37*, 6376.
(22) Fu, G. D.; Shang, Z. H.; Hong, L.; Kang, E. T.; Neoh, K. G. *Macromolecules* **2005**, *38*, 7867.
(23) Ohno, K.; Morinaga, T.; Koh, K.; Tsujii, Y.; Fukuda, T. *Macromolecules* **2005**, *38*, 2137.
(24) Li, D. J.; Sheng, X.; Zhao, B. *J. Am. Chem. Soc.* **2005**, *127*, 6248.
(25) Carrot, G.; El Harrak, A.; Oberdisse, J.; Jestin, J.; Boue, F. *Soft Matter* **2006**, *2*, 1043.
(26) Li, D. J.; Jones, G. L.; Dunlap, J. R.; Hua, F. J.; Zhao, B. *Langmuir* **2006**, *22*, 3344.
(27) Morinaga, T.; Ohkura, M.; Ohno, K.; Tsujii, Y.; Fukuda, T. *Macromolecules* **2007**, *40*, 1159.
(28) Zhang, K.; Ma, J.; Zhang, B.; Zhao, S.; Li, Y. P.; Xu, Y. X.; Yu, W. Z.; Wang, J. Y. *Mater. Lett.* **2007**, *61*, 949.
(29) Tsujii, Y.; Ejaz, M.; Sato, K.; Goto, A.; Fukuda, T. *Macromolecules* **2001**, *34*, 8872.
(30) Li, C. Z.; Benicewicz, B. C. *Macromolecules* **2005**, *38*, 5929.
(31) Li, C.; Han, J.; Ryu, C. Y.; Benicewicz, B. C. *Macromolecules* **2006**, *39*, 3175.
(32) Zhao, Y. L.; Perrier, S. *Macromolecules* **2006**, *39*, 8603.
(33) Blomberg, S.; Ostberg, S.; Harth, E.; Bosman, A. W.; Van Horn, B.; Hawker, C. J. *J. Polym. Sci., Part A: Polym. Chem.* **2002**, *40*, 1309.
(34) Bartholome, C.; Beyou, E.; Bourgeat-Lami, E.; Chaumont, P.; Zydowicz, N. *Macromolecules* **2003**, *36*, 7946.
(35) Julien Parvole, G. L. A. K. L. B. *Macromol. Chem. Phys.* **2005**, *206*, 372.
(36) Bartholome, C.; Beyou, E.; Bourgeat-Lami, E.; Chaumont, P.; Lefebvre, F.; Zydowicz, N. *Macromolecules* **2005**, *38*, 1099.
(37) Schild, H. G. *Prog. Polym. Sci.* **1992**, *17*, 163.
(38) Shan, J.; Nuopponen, M.; Jiang, H.; Kauppinen, E.; Tenhu, H. *Macromolecules* **2003**, *36*, 4526.
(39) Raula, J.; Shan, J.; Nuopponen, M.; Niskanen, A.; Jiang, H.; Kauppinen, E. I.; Tenhu, H. *Langmuir* **2003**, *19*, 3499.
(40) Shan, J.; Chen, J.; Nuopponen, M.; Tenhu, H. *Langmuir* **2004**, *20*, 4671.
(41) Rademacher, J. T.; Baum, R.; Pallack, M. E.; Brittain, W. J.; Simonsick, W. J. *Macromolecules* **2000**, *33*, 284.
(42) Teodorescu, M.; Matyjaszewski, K. *Macromolecules* **1999**, *32*, 4826.
(43) Kim, D. J.; Kang, S. M.; Kong, B.; Kim, W. J.; Paik, H. J.; Choi, H.; Choi, I. S. *Macromol. Chem. Phys.* **2005**, *206*, 1941.
(44) Braunecker, W. A.; Matyjaszewski, K. *Prog. Polym. Sci.* **2007**, *32*, 93.
(45) Jewrajka, S. K.; Mandal, B. M. *Macromolecules* **2003**, *36*, 311.
(46) Masci, G.; Giacomelli, L.; Crescenzi, V. *Macromol. Rapid Commun.* **2004**, *25*, 559.

Several research groups have attempted to conduct the ATRP of acrylamido monomers in a controlled manner. In 2000, Matyjaszewski et al.[47] successfully synthesized poly(*N*, *N*-dimethylacrylamide) (PDMA) with low polydispersity employing methyl 2-chloropropionate as the initiator and CuCl/tris(2-(dimethylamino)ethyl)amine (Me_6TREN) as the catalysts. Masci et al.[46] prepared PNIPAM with low polydispersity via ATRP in DMF/water mixtures using CuCl/Me_6TREN as the catalyst. Stöver et al.[48] further proved that NIPAM can be controllably polymerized in various alcohols at ambient temperature by ATRP under similar conditions.

On the other hand, the thermal phase transition behavior of thermoresponsive PNIPAM brushes at the surface of hybrid nanoparticles is also an interesting but still controversial topic. Theoretical predictions suggest that the collapse of surface-tethered polymer brushes accompanying a solubility transition proceeds continuously over a much broader range as the solvent quality decreases,[49–51] which are distinct from those of free flexible chains adopting random-coil conformations in solution.[52] Balamurugan et al.[53] used surface plasmon resonance (SPR) spectroscopy and contact angle measurements to study the phase transitions of PNIPAM brushes grafted from a self-assembled monolayer on bulk gold surface. They concluded that polymer segments in the outermost region of brushes remain solvated until the LCST of ~32 °C, while densely packed segments within the brush layer collapse over a broad temperature range of 10–40 °C.

Tenhu et al.[40] employed the "grafting to" approach to prepare hybrid gold nanoparticles surface coated with PNIPAM brushes with a grafting density of 0.42 nm^2 per chain, starting from thiol-terminated PNIPAM chains prepared via the RAFT process. They observed intriguing double thermal phase transitions at ~30 and 40 °C as revealed by microdifferential scanning calorimetry (micro-DSC). However, two uncertainties remained for this fascinating system. First, PNIPAM chains were terminated with either a hydrophobic cumyl or a hydrophilic carboxyl group, and the nature of end groups may significantly affect the phase transition of PNIPAM brushes. Even for PNIPAM homopolymers in aqueous solution, they observed asymmetric endothermic micro-DSC peaks, and the presence of a shoulder at higher temperatures was clearly discernible. Second, the gold nanoparticle cores were quite small (~1–2 nm); thus, these hybrid nanoparticles more resembled to star polymers rather than polymer brush-coated ones.

To further explore the thermal phase transition behavior of PNIPAM brushes at the surface of inorganic nanoparticles and exclude the interference from end groups and free PNIPAM chains, hybrid silica nanoparticles coated with PNIPAM brushes prepared by surface-initiated ATRP would be highly desirable due to following advantages: polymer brushes are covalently attached to silica cores, the ATRP surface grafting mechanism can exclude the formation of free nongrafted PNIPAM chains, and the hydrophobicity of terminal halogen groups can be safely neglected.

In this communication, we explored the surface-initiated ATRP of NIPAM in 2-propanol from silica nanoparticles derivatized with ATRP initiators, employing CuCl/$CuCl_2$/Me_6TREN as catalysts. The polymerization kinetics and the evolution of number-average molecular weights, M_n, and polydispersities, M_w/M_n, with monomer conversions were investigated. We successfully demonstrated that the ATRP of NIPAM at the surface of silica nanoparticles can be conducted in a well-controlled manner, leading to hybrid nanoparticles with PNIPAM brushes of tunable thickness. The thermal phase transitions of PNIPAM brushes were further investigated via a combination of LLS and turbidimetry, and the results were compared to those obtained for PNIPAM brushes at the surface of hybrid gold nanoparticles.[40]

Experimental Section

Materials. *N*-Isopropylacrylamide (NIPAM, 97%, Tokyo Kasei Kagyo Co.) was purified by recrystallization from the mixture of benzene and *n*-hexane (1/3, v/v). CuCl (99.999%), $CuCl_2$ (99%), and 2-bromoisobutyryl bromide (97%) were purchased from Aldrich and used without further purification. Tetraethoxysilane (TEOS) and 3-aminopropyltriethoxysilane (APTES) were purchased from Silicone Materials Co. (Wuhan University) and distilled under reduced pressure just prior to use. Tris(2-(dimethylamino)ethyl)amine (Me_6TREN) was synthesized according to literature procedures.[54] All other reagents were purchased from Sinopharm Chemical Reagent Co. Ltd. and used as received.

Sample Preparation. The general approaches to the preparation of amino-functionalized, 2-bromoisobutyrate-functionalized, and thermoresponsive PNIPAM grafted silica nanoparticles are shown in Scheme 1.

Synthesis of Bare Silica Nanoparticles. Ammonium hydroxide (25 wt % in water, 25 mL) and ethanol (500 mL) were added into a two-necked round-bottom flask at ambient temperature; the mixture was stirred at a speed of 300 rpm. A mixture of tetraethoxysilane (TEOS, 12.5 mL) and ethanol (14 mL) was added into the flask at a rate of ~1 mL/min via a dropping funnel. The concentrations of NH_3, H_2O, and TEOS in the final mixture were ca. 0.6, 1.7, and 0.1 M, respectively. After stirring for 20 h at room temperature, the nanoparticles were isolated by centrifugation at 8000 rpm. After discarding the supernatant, the sediments were redispersed in ethanol and centrifugated again. This purification cycle was repeated for four times. The obtained nanoparticles were then dispersed and stored in 50 mL of ethanol.

Synthesis of Amino-Functionalized Silica Nanoparticles. The above ethanol suspension of bare silica nanoparticles (45 mL) was transferred into a 100 mL flask equipped with a magnetic stir bar. After heating to 60 °C, ammonium hydroxide (25 wt % in water, 50 μL) was injected into the flask. APTES (0.4 mL, 1.7 mmol) was added dropwise. The reaction mixture was stirred at 60 °C for 12 h and then cooled to room temperature. The nanoparticles were

(47) Teodorescu, M.; Matyjaszewski, K. *Macromol. Rapid Commun.* **2000**, *21*, 190.
(48) Xia, Y.; Yin, X. C.; Burke, N. A. D.; Stover, H. D. H. *Macromolecules* **2005**, *38*, 5937.
(49) Szleifer, I.; Carignano, M. A. Tethered polymer layers. In *Advances in Chemical Physics*; John Wiley & Sons: New York, 1996; Vol. 94, p 165.
(50) Wagner, M.; Brochardwyart, F.; Hervet, H.; Degennes, P. G. *Colloid Polym. Sci.* **1993**, *271*, 621.
(51) Zhulina, E. B.; Borisov, O. V.; Pryamitsyn, V. A.; Birshtein, T. M. *Macromolecules* **1991**, *24*, 140.
(52) Teraoka, I. *Polymer Solutions: An Introduction to Physical Properties*; John Wiley & Sons: New York, 2002.
(53) Balamurugan, S.; Mendez, S.; Balamurugan, S. S.; O'Brien, M. J.; Lopez, G. P. *Langmuir* **2003**, *19*, 2545.
(54) Ciampolini, M.; Nardi, N. *Inorg. Chem.* **1966**, *5*, 41.

Scheme 1. Schematic illustration of the synthesis of hybrid silica nanoparticles coated with thermoresponsive poly(*N*-isopropylacrylamide) (PNIPAM) brushes via surface-initiated atom transfer radical polymerization (ATRP). The densely grafted PNIPAM brushes exhibit reversible thermosensitive swelling/collapse phase transitions

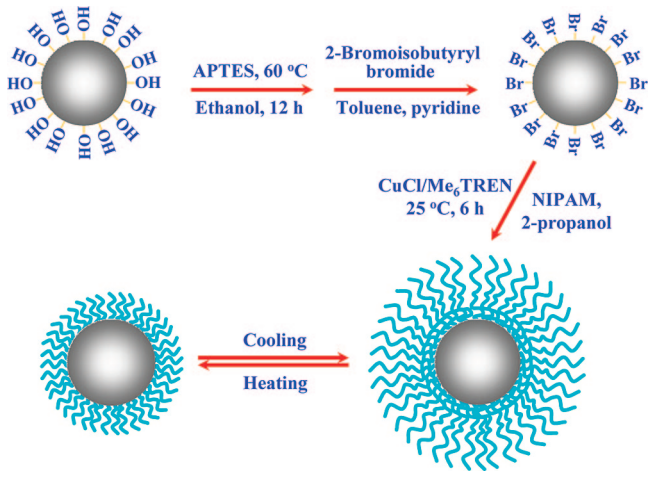

isolated by centrifugation at 8000 rpm. After discarding the supernatant, the sediments were redispersed in toluene and centrifugated again. The above purification cycle was repeated for three times to remove excess APTES. The amino-functionalized silica nanoparticles were finally redispersed in 50 mL of anhydrous toluene.

Synthesis of 2-Bromoisobutyrate-Functionalized Silica Nanoparticles. The above toluene suspension of amino-functionalized silica nanoparticles (45 mL) was mixed with dry pyridine (0.3 mL, 3.7 mmol) in a flask. After cooling to 0 °C, 2-bromoisobutyryl bromide (0.25 mL, 2.0 mmol) was added dropwise. The solution was stirred at 0 °C for 0.5 h and then at room temperature for 12 h. The nanoparticles were purified and isolated following similar procedures as those described for the synthesis of amino-functionalized silica nanoparticles.The final product was dried in a vacuum oven overnight at 50 °C.

Surface-Initiated ATRP of NIPAM from Initiator-Functionalized Silica Nanoparticles. Initiator-functionalized silica nanoparticles (300 mg, 0.051 mmol of initiating sites), Me_6TREN (62 mg, 0.27 mmol), $CuCl_2$(3.4 mg, 0.025 mmol), NIPAM (0.625 g, 5.52 mmol), and 2-propanol (4 mL) were added to a Schlenk flask equipped with a magnetic stir bar. The silica nanoparticles were dispersed by ultrasonication. The mixture was degassed by three freeze–pump–thaw cycles. In the frozen state, CuCl (25 mg, 0.25 mmol) was added under protection of N_2 flow. The flask was then subjected to two additional freeze–pump–thaw cycles and then placed at ambient temperature (25 °C). Stirring was started immediately after thawing. During polymerization, an aliquot of the reaction mixture (0.2 mL) was withdrawn at predetermined time intervals, which was exposed to air and divided into two parts. One part was roughly dried under gentle N_2 flow and dispersed in $CDCl_3$ for the determination of monomer conversions by ^1H NMR analysis. The remaining part was subjected to centrifugation and then treated with hydrofluoric acid to cleave the grafted PNIPAM chains for further GPC analysis.

After 6 h, the flask was exposed to air to terminate the polymerization. Nanoparticles were isolated via centrifugation at 10 000 rpm, redispersion in ethanol, and centrifugation again. This purification cycle was repeated for three times, and the obtained PNIPAM-grafted nanoparticles were dried in a vacuum oven overnight at 50 °C. The supernatant solutions during purification were combined and concentrated on a rotary evaporator. The absence of free nongrafted PNIPAM chains during surface-initiated ATRP can be apparently confirmed by the fact that adding a large excess of ethyl ether (nonsolvent for PNIPAM) into the concentrated supernatants resulted in a clear dispersion.

Characterization. *Gel Permeation Chromatography (GPC).* Molecular weights and molecular weight distributions were determined by a gel permeation chromatograph (GPC) equipped with a Waters 1515 pump and a Waters 2414 differential refractive index detector (set at 30 °C). It uses a series of three linear Styragel columns HT2, HT4, and HT5 at an oven temperature of 45 °C. The eluent was THF at a flow rate of 1.0 mL/min. A series of low-polydispersity polystyrene standards were employed for the GPC calibration.

Fourier Transform Infrared Spectroscopy (FT-IR). Fourier transform infrared (FT-IR) spectra were recorded on a Bruker VECTOR-22 IR spectrometer. The spectra were collected at 64 scans with a spectral resolution of 4 cm^{-1}.

Thermogravimetric Analysis (TGA). TGA was performed in air at a heating rate of 10 °C/min from room temperature to 800 °C using a Perkin-Elmer Diamond TG/DTA.

Transmission Electron Microscopy (TEM). TEM observations were conducted on a Philips CM 120 electron microscope at an acceleration voltage of 100 kV. The sample for TEM observations was prepared by placing a 10 μL nanoparticle solution on copper grids successively coated with thin films of Formvar and carbon. No staining was required.

Laser Light Scattering (LLS). A commercial spectrometer (ALV/DLS/SLS-5022F) equipped with a multitau digital time correlator (ALV5000) and a cylindrical 22 mW UNIPHASE He–Ne laser (λ_0 = 632 nm) as the light source was employed for dynamic and static LLS measurements. In dynamic LLS, scattered light was collected at a fixed angle of 90° for a duration of 15 min. Distribution averages and particle size distributions were computed using cumulants analysis and CONTIN routines. All data were averaged over three measurements.

In static LLS, we can obtain the weight-average molar mass (M_w) and the z-average root-mean-square radius of gyration ($\langle R_g^2 \rangle^{1/2}$ or written as $\langle R_g \rangle$) of polymer chains or aggregates in a dilute solution from the angular dependence of the excess absolute scattering intensity, known as Rayleigh ratio $R_{vv}(q)$. The specific refractive index increments (dn/dc) were determined by a precise differential refractometer at 632 nm. The molar mass of PNIPAM grafted silica nanoparticles was measured at only one concentration (5×10^{-6} g/mL), and the extrapolation to zero concentration was not conducted. Thus, the obtained M_w should only be considered as apparent values, denoted as $M_{w,app}$.

Optical Transmittance Measurements. The optical transmittance of aqueous solutions of hybrid nanoparticles was acquired at a wavelength of 800 nm on a Unico UV/vis 2802PCS spectrophotometer using a thermostatically controlled cuvette.

Micro-Differential Scanning Calorimetry (Micro-DSC) Characterization. Micro-DSC measurements were carried on a VP DSC from MicroCal. The volume of the sample cell was 0.509 mL. The reference cell was filled with deionized water. The sample solution with a concentration of 1.0 g/L was degassed at 25 °C for half an hour and equilibrated at 10 °C for 2 h before heating at a rate of 1.0 °C/min.

Results and Discussion

The general approach to the preparation of thermoresponsive PNIPAM grafted silica nanoparticles is shown in Scheme 1.

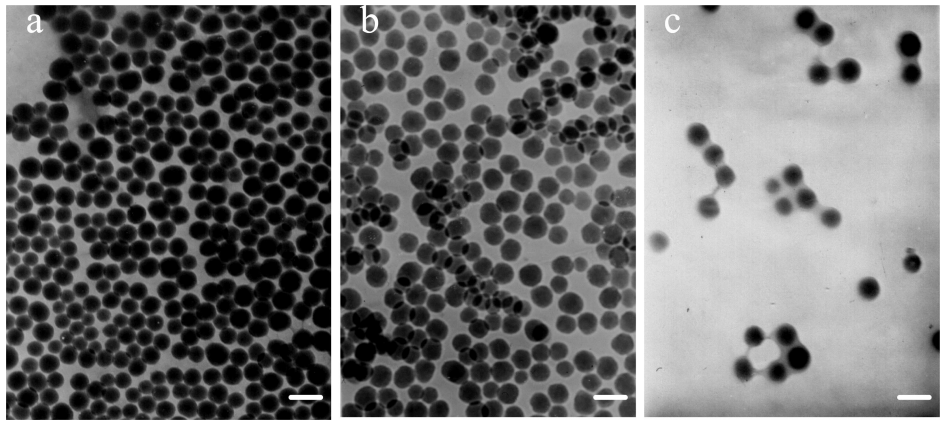

Figure 1. TEM images of (a) bare silica nanoparticles, (b) 2-bromoisobutyrate-functionalized silica nanoparticles, and (c) hybrid silica nanoparticles coated with thermoresponsive PNIPAM brushes obtained by surface-initiated ATRP (6 h, 29% monomer conversion). Scale bar: 100 nm.

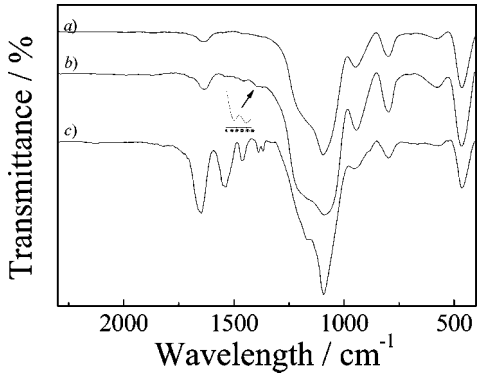

Figure 2. Fourier transform infrared (FT-IR) spectra of (a) bare silica nanoparticles, (b) 2-bromoisobutyrate-functionalized silica nanoparticles, and (c) hybrid silica nanoparticles coated with thermoresponsive PNIPAM brushes obtained by surface-initiated ATRP.

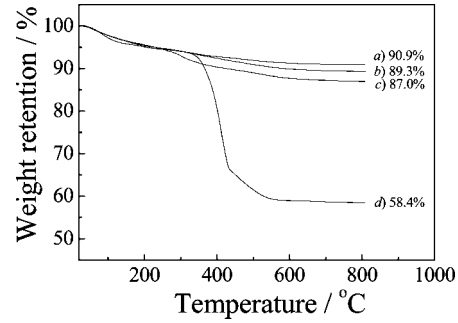

Figure 3. Thermogravimetric analysis (TGA) of (a) bare silica nanoparticles, (b) amino-functionalized silica nanoparticles, (c) 2-bromoisobutyrate-functionalized silica nanoparticles, and (d) hybrid silica nanoparticles coated with thermoresponsive PNIPAM brushes obtained by surface-initiated ATRP. TGA was performed in air at a heating rate of 10 °C/min.

Synthesis of ATRP Initiator-Functionalized Silica Nanoparticles. Bare silica nanoparticles were prepared using the Stöber process,[55] which has been well-known to produce spherical silica nanoparticles with relatively narrow size distributions. In this study, silica nanoparticles with an average diameter of ~70 nm, as determined by TEM (Figure 1a), were used to fabricate thermosensitive hybrid silica nanoparticles. The surface functional groups of bare silica nanoparticles, i.e., silanol (Si–OH) and ethoxy (Si–O–C_2H_5),[56] were converted to primary amine groups by treating with APTES. 2-Bromoisobutyrate-functionalized silica nanoparticles were then prepared via reacting amino-functionalized silica nanoparticles with 2-bromoisobutyryl bromide. The average diameter of the initiator-functionalized silica nanoparticles is ~70 nm (Figure 1b), which is identical to that obtained for bare silica nanoparticles (Figure 1a).

FT-IR was employed to verify the successful amidation of amino-functionalized silica nanoparticles with 2-bromoisobutyryl bromide. For bare silica nanoparticles (Figure 2a), absorption peaks characteristic of tetrahedron silica structures occur at 1100 cm^{-1} (Si–O stretching) and 465 cm^{-1} (Si–O bending). We can also observe the Si–OH bending at 945 cm^{-1} and the Si–O–Si bending at 800 cm^{-1}. After amidation, a doublet at 1390 and 1370 cm^{-1}, where were characteristic of the deformation of two methyl groups in 2-bromoisobutyrate residues, can be clearly discerned (Figure 2b).

The attachment of 2-bromoisobutyryl moieties can be further proved by TGA analysis. There exists ~2.3 wt % difference in the weight retentions at 800 °C between amino- and 2-bromoisobutyrate-functionalized silica nanoparticles (Figure 3b,c). If the mass retention of amino-functionalized silica nanoparticles at 800 °C is used as the reference and the density of the silica nanoparticles is assumed to be identical to that of bulk silica (2.07 g/cm^3), we can roughly estimate the grafting density of ATRP initiators at the surface of silica nanoparticles (70 nm in diameter) to be ~0.35 nm^2/initiator.

Surface-Initiated ATRP of NIPAM from 2-Bromoisobutyrate-Functionalized Silica Nanoparticles. ATRP of NIPAM at the surface of initiator-functionalized silica nanoparticles was conducted in 2-propanol at ambient temperature, using CuCl/$CuCl_2$ and Me_6TREN as the catalytic system. $CuCl_2$ (10 mol % relative to CuCl) was added in order to ensure an efficient exchange between the dormant and active species. For the ATRP of NIPAM in a homogeneous media as those reported by Masci et al.[46] and Stöver et al.,[48] the addition of Cu(II) is unnecessary. In surface-initiated ATRP, the number of initiators at the surface of silica cores is inadequate to generate enough Cu(II) species, especially at the early stages. Thus, once radicals are generated, they cannot easily

(55) Stober, W.; Fink, A.; Bohn, E. *J. Colloid Interface Sci.* **1968**, *26*, 62.
(56) Badley, R. D.; Ford, W. T.; McEnroe, F. J.; Assink, R. A. *Langmuir* **1990**, *6*, 792.

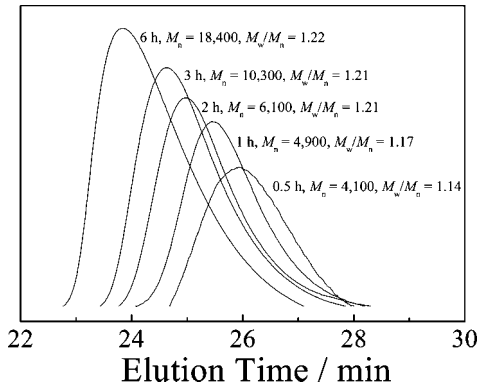

Figure 4. Evolution of GPC traces with polymerization time during the surface-initiated atom transfer radical polymerization of NIPAM from 2-bromoisobutyrate-functionalized silica nanoparticles. The PNIPAM brushes were cleaved from silica nanoparticles via etching with hydrofluoric acid.

revert to their dormant state, leading to unavoidable radical coupling. This issue can be solved by the addition of low concentration of Cu(II) species at the beginning of surface-initiated ATRP polymerization.[14,57,58]

Monomer conversions were monitored by ^{1}H NMR based on the integration areas of resonance peaks at 4.0 ppm (1H, characteristic of NIPAM monomer and PNIPAM polymer) and 6.0–6.4 ppm (2H, vinyl protons of NIPAM monomer). Portions of samples taken at time intervals during polymerization were also subjected to centrifugation and then treated with hydrofluoric acid to cleave the grafted PNIPAM chains for GPC analysis. The time evolution of number-average molecular weight, M_n, and molecular weight distributions, M_w/M_n, was obtained for cleaved PNIPAM chains by GPC analysis. Typical GPC traces of grafted PNIPAM chains at increasing monomer conversions are shown in Figure 4. We can clearly observe that the elution peaks shift to higher molecular weight with the increase of polymerization time. After 6 h, the monomer conversion is ~29%; GPC analysis of the cleaved PNIPAM chains reveals a number-average molecular weight, M_n, of 18 400 and a polydispersity, M_w/M_n, of 1.22. The GPC elution peak of grafted PNIPAM exhibits a discernible tailing at the lower molecular weight side, probably due to premature chain termination during polymerization.

The kinetic plots for the surface-initiated ATRP of NIPAM are shown in Figure 5a, exhibiting linear first-order kinetics. From Figure 5b, we could clearly observe the linear increase of M_n with monomer conversions. Moreover, the polydispersity values remained narrow throughout the polymerization (<1.25). The linear increase of M_n with monomer conversions and the quite linear kinetic plot suggested that the surface-initiated ATRP of NIPAM from silica nanoparticles could be conducted in a controlled manner under the current conditions.

Figure 1c shows the TEM image of PNIPAM grafted hybrid silica nanoparticles; it is clearly evident that silica

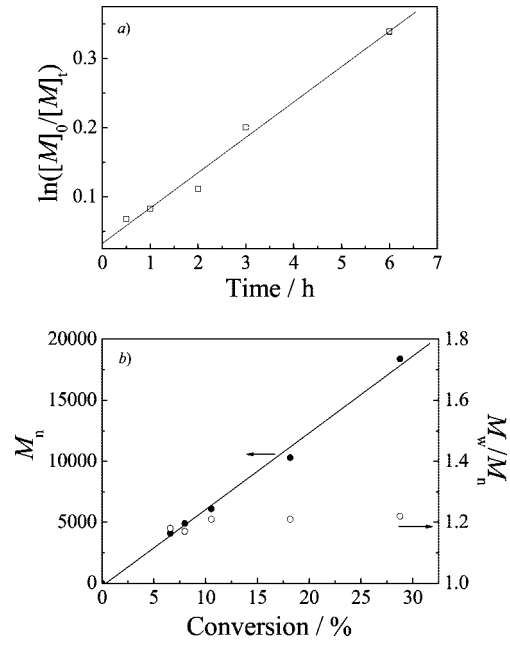

Figure 5. (a) Kinetic plot and (b) evolution of molecular weights (●) and polydispersities, M_w/M_n (○), with monomer conversions obtained during surface-initiated ATRP of NIPAM.

cores are surrounded by a polymer layer. Figure 2c shows the FT-IR spectrum of hybrid silica nanoparticles grafted with PNIPAM chains obtained by surface-initiated ATRP for 6 h (29% monomer conversion). We can clearly observe the amide I band (1648 cm^{-1}, C═O stretching) and amide II band (1538 cm^{-1}, N–H stretching). The presence of two bands at 1367 and 1388 cm^{-1} with almost equal intensity are associated with the deformation of two methyl groups on isopropyl.[59]

From the TGA results (Figure 3d), the weight retention at 800 °C obtained for PNIPAM-grafted silica nanoparticles at 29% monomer conversion is ~58.4%. Using the weight retention at 800 °C (87.0 wt %) obtained for 2-bromoisobutyrate-functionalized silica nanoparticles as a reference, the PNIPAM weight content relative to that of silica cores was calculated to be ~56.2%. As the M_n of grafted PNIPAM chains was determined to be 18 400 by GPC, the grafting density of PNIPAM chains at the surface of silica nanoparticles can be estimated to be ~2.2 nm^2/chain, which is relatively high. As the grafting density of ATRP initiators at the surface of silica nanoparticles was 0.35 nm^2/initiator, the initiator efficiency for the surface-initiated ATRP of NIPAM can be estimated to be ~16%. Thus, the theoretical degree of polymerization (DP) of grafted PNIPAM chains can be estimated to be ~200 on the basis of monomer conversion (29%) and the calculated initiator efficiency (16%). This generally agrees with the actual DP of grafted PNIPAM (~160) obtained from GPC analysis.

LLS Characterization. Dynamic and static LLS were used to characterize the size and size distribution of hybrid silica nanoparticles grafted with PNIPAM chains (6 h polymerization time, 29% monomer conversion) in aqueous solution at different temperatures. It is well-known that

(57) Kim, J. B.; Huang, W. X.; Miller, M. D.; Baker, G. L.; Bruening, M. L. *J. Polym. Sci., Part A: Polym. Chem.* **2003**, *41*, 386.
(58) Matyjaszewski, K.; Miller, P. J.; Shukla, N.; Immaraporn, B.; Gelman, A.; Luokala, B. B.; Siclovan, T. M.; Kickelbick, G.; Vallant, T.; Hoffmann, H.; Pakula, T. *Macromolecules* **1999**, *32*, 8716.
(59) Pan, Y. V.; Wesley, R. A.; Luginbuhl, R.; Denton, D. D.; Ratner, B. D. *Biomacromolecules* **2001**, *2*, 32.

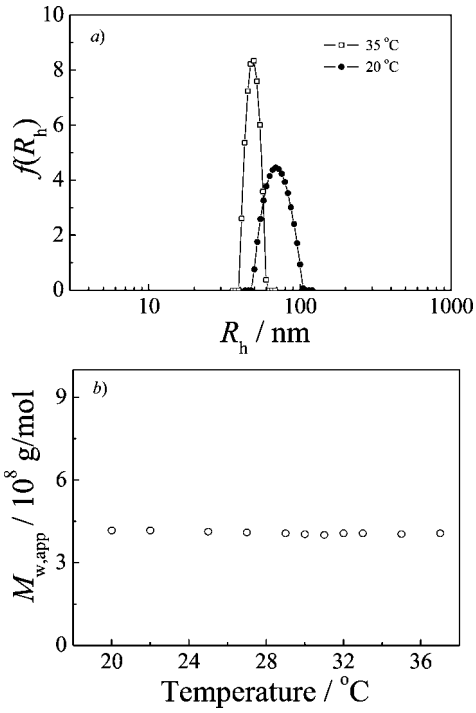

Figure 6. Temperature dependence of (a) typical hydrodynamic radius distributions, $f(R_h)$, and (b) apparent molar masses, $M_{w,app}$, obtained for 5 $\times$ 10^{-6} g/mL aqueous solution of hybrid silica nanoparticles coated with thermoresponsive PNIPAM brushes.

PNIPAM homopolymer undergoes a coil-to-globule phase transition in dilute aqueous solution at its LCST of ca. 32 °C.[37] At temperatures below the LCST, PNIPAM chains adopt a random-coil conformation, while at temperatures above the LCST, intramolecular hydrogen-bonding interactions between C═O and N–H groups render the chains to collapse and compact, reducing their water solubility.

Figure 6a shows typical hydrodynamic radius distributions, $f(R_h)$, of PNIPAM grafted silica nanoparticles at different temperatures. At 20 °C, R_h is in the range 48–105 nm, with an average hydrodynamic radius, $\langle R_h \rangle$, of 69 nm. Upon heating to 35 °C, R_h ranges from 39 to 62 nm with a $\langle R_h \rangle$ of 48 nm. We can calculate that the hydrodynamic volume of the PNIPAM layer shrinks ~4.2 times upon heating from 20 to 35 °C. The decrease of nanoparticle sizes at elevated temperature should be ascribed to the collapse of PNIPAM chains above its thermal phase transition temperature. The polydispersity indexes of nanoparticle size distributions (μ_2/Γ^2) are 0.04 and 0.01 at 20 and 35 °C, respectively. This indicates that the obtained hybrid nanoparticles are quite monodisperse in size, which is in agreement with TEM results as shown in Figure 1c. Moreover, further LLS studies reveal that the swelling and collapse of PNIPAM brushes of hybrid silica nanoparticles are fully reversible upon cycling the solution temperature between 20 and 35 °C.

The dn/dC value of the aqueous solution of hybrid silica nanoparticles was determined to be 0.178 mL/g at 20 °C, which is quite comparable to that of PNIPAM homopolymer in water. The same dn/dC value was used at all temperatures, assuming that the temperature effect on dn/dC values is negligible. Figure 6b shows the temperature dependence of apparent molar mass, $M_{w,app}$, of PNIPAM-grafted silica nanoparticles. We can clearly see from Figure 6b that $M_{w,app}$ remains constant at ~4.1 $\times$ 10^8 g/mol over the temperature range 20–37 °C. This indicates that at a quite low concentration of 5 $\times$ 10^{-6} g/mL used for LLS there is no apparent aggregation between PNIPAM-grafted silica nanoparticles. Above the thermal phase transition temperature of PNIPAM brushes, PNIPAM chains in the grafted layer only collapse and aggregate within each core–shell nanoparticles (Scheme 1).

Assuming an average density of 2.07 g/cm^3 for silica cores (70 nm in diameter), the molar mass of silica cores can be calculated to be 2.24 $\times$ 10^8 g/mol. We can then calculate that on average ~8300 PNIPAM chains were grafted per silica nanoparticle, considering that the weight-average molecular weight of grafted PNIPAM chains is ~22 400. The surface grafting density of PNIPAM chains can be estimated to be ~1.85 nm^2/chain, which is generally in agreement with that obtained from TGA results (Figure 3).

Moreover, the average distance between neighboring grafted PNIPAM chains at the surface of silica nanoparticles is calculated to be ~1.4 nm. The DP of grafted PNIPAM chains is ca. 160, as determined by GPC analysis in THF (Figure 4). Preliminary experiments revealed that the $\langle R_h \rangle$ value of free PNIPAM chain with a DP of ~160 in aqueous solutions is ~3–4 nm. Thus, the hydrodynamic dimensions (6–8 nm) of free PNIPAM chains are much larger than the average distance between neighboring grafted PNIPAM chains with comparable DP (~1.4 nm) at the surface of silica nanoparticles. This indicates that the grafted PNIPAM layer falls into the brush regime; i.e., the distance between grafted sites is much less than the size of polymer coils. PNIPAM chains in the brushes are crowded and forced to stretch away from the substrate due to steric exclusion between neighboring chains (Scheme 1).

This was further confirmed by LLS results. The radius of the silica core was about 35 nm (Figure 1a), and the thickness of PNIPAM brushes at 20 °C was estimated to be 34 nm. So the dimension of PNIPAM chains in the brush is much larger than that of the free PNIPAM chains with the same DP in solution (~6–8 nm). On the other hand, the calculated end-to-end distance of fully extended PNIPAM chain with a DP of 160 is ca. 40 nm. This indicates that the surface attached PNIPAM chains are almost fully extended due to steric exclusions imposed by neighboring chains in the PNIPAM brush. The dynamic LLS results agree favorably with those obtained from PNIPAM stabilized PS latex nanoparticles, in which chain stretching was also observed.[60]

Double Thermal Phase Transitions. Figure 7 shows the temperature dependence of average hydrodynamic radius, $\langle R_h \rangle$, and average radius of gyration, $\langle R_g \rangle$, of PNIPAM-grafted silica nanoparticles in aqueous solution. The results apparently tell us that thermal phase transitions of PNIPAM brushes at the surface of silica nanoparticles spanned a broad temperature range. Upon heating, $\langle R_h \rangle$ decreases monotonically from 69 to 63 nm in the temperature range 20–29 °C and then exhibits a further decrease from 61 nm at 31 °C to 47 nm at 37 °C.

(60) Kizhakkedathu, J. N.; Norris-Jones, R.; Brooks, D. E. *Macromolecules* **2004**, *37*, 734.

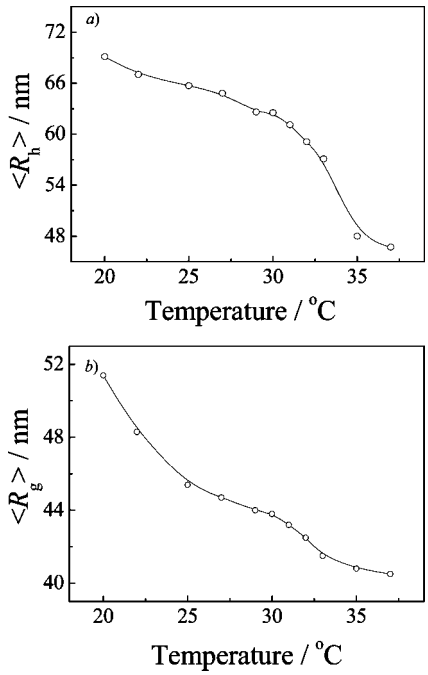

Figure 7. Temperature dependence of (a) intensity-average hydrodynamic radius, $\langle R_h \rangle$, and (b) average radius of gyration, $\langle R_g \rangle$, obtained for 5×10^{-6} g/mL aqueous solution of hybrid silica nanoparticles coated with PNIPAM brushes.

$\langle R_g \rangle$ is very sensitive to segment density distributions for polymer chains and core/shell nanoparticles. The temperature dependence of $\langle R_g \rangle$ clearly reveals that PNIPAM brushes grafted on silica cores undergo a two-stage collapse. $\langle R_g \rangle$ is ca. 51 nm at 20 °C. Upon heating, it gradually decreases to 44 nm at 29 °C and then reaches a plateau region in the temperature range 29–30 °C. Above 31 °C, $\langle R_g \rangle$ further decreases from 43 to 40 nm in the temperature range 31–37 °C.

Previously, we fabricated hybrid nanoparticles coated with PNIPAM brushes via the self-assembling approach, starting from poly(*N*-isopropylacrylamide)-*b*-poly(γ-methacryloxypropyltrimethoxysilane) (PNIPAM-*b*-PMPS).[61] The grafting density of PNIPAM chains at the nanoparticle surface is ~6.7 nm^2/chain. LLS studies also revealed that both $\langle R_g \rangle$ and $\langle R_h \rangle$ exhibit a two-stage collapse. In another example,[62] PNIPAM chains were grafted from hydrophobic hyperbranched polyester (~3 nm in diameter) via the RAFT process. Both micro-DSC and LLS revealed double phase transitions; one occurred in the lower temperature range of 20–30 °C, and the other occurred above 30 °C.

Tenhu et al.[40] grafted PNIPAM chains with hydrophobic cumyl or hydrophilic carboxyl end groups from gold nanoparticles with a diameter of 1–2 nm, the DP of grafted PNIPAM chains is ~40–50, and the grafting density is very high (~0.4 nm^2/chain). There are ~30 PNIPAM chains at the surface of gold nanoparticles. Microcalorimetric measurements revealed two well-separated phase transitions at ~30 and 40 °C. They also found that the phase transitions of PNIPAM brushes were obviously affected by the end group of grafted PNIPAM chains. Even for PNIPAM homopolymers in aqueous solution, they observed asymmetric endothermic micro-DSC peaks and the presence of a shoulder peak at higher temperatures.[40]

Stöver et al.[63] recently studied the end-group effects on the thermal phase transitions of narrow-disperse PNIPAM samples. They concluded that for low molecular weight samples the hydrophobicity/hydrophilicity of end groups exhibits significant effects, whereas for PNIPAM with an $M_n > 10$ kDa, the end-group effects rapidly diminish. In our case, PNIPAM chains were terminated with halogen groups, and their hydrophobicity can be neglected. Moreover, the M_n of grafted PNIPAM chains is well above 10 kDa. Figure S1 of the Supporting Information shows the micro-DSC results of PNIPAM chains cleaved from hybrid silica nanoparticles, which clearly revealed the presence of a monomodal and relatively sharp endothermic peak. Thus, the different double phase transition temperatures observed for PNIPAM-grafted silica nanoparticles as compared to those obtained by Tenhu et al.[40] should be ascribed to the differences in M_n of grafted PNIPAM chains and the end-group effects.

Tenhu et al.[40] ascribed the double phase transitions to the differences in local concentrations in the inner and outer region of PNIPAM brushes. The fraction of PNIPAM segments in the inner region was higher than that in the outer part. Afroze et al.[64] deduced that phase transition temperatures of PNIPAM decrease with increasing PNIPAM concentrations, up to the mass fraction of 0.5. Thus, the inner zone of PNIPAM brushes possesses a lower phase transition temperature than that of the outer zone.

In our case, silica nanoparticles were coated with PNIPAM chains with a DP of ~160, the size of silica cores is ~35 nm, and the thickness and overall molar mass of PNIPAM brushes at 20 °C are 34 nm and 1.86×10^8 g/mol (Figure 6), respectively. The overall density of PNIPAM layer can be calculated to be ~0.26 g/cm^3. On the other hand, as the PNIPAM chains were grafted in a radial manner from spherical silica nanoparticles, we can roughly estimate that the local chain density can be as high as 0.57 g/cm^3 for the innermost zone (1 nm thickness) of PNIPAM brushes, whereas for the outermost zone (1 nm thickness), it is 0.15 g/cm^3.

The double phase transitions can be further explained by invoking the *n*-clusters concept developed by de Gennes.[50] According to this idea, chain segments in the inner zone of polymer brushes can exhibit attractive *n*-body interactions while the two-body interactions are still weakly repulsive, initiating the collapse of chain segments densely packed in the inner zone. Theoretically, this will more abruptly decrease $\langle R_g \rangle$ compared to that for $\langle R_h \rangle$. This partially explains that in Figure 7 the two-stage decrease of $\langle R_g \rangle$ is more clearly evident than that obtained for $\langle R_h \rangle$ in the temperature range of 20–37 °C.

(61) Zhang, Y. F.; Luo, S. Z.; Liu, S. Y. *Macromolecules* **2005**, *38*, 9813.
(62) Luo, S. Z.; Xu, J.; Zhu, Z. Y.; Wu, C.; Liu, S. Y. *J. Phys. Chem. B* **2006**, *110*, 9132.
(63) Xia, Y.; Burke, N. A. D.; Stover, H. D. H. *Macromolecules* **2006**, *39*, 2275.
(64) Afroze, F.; Nies, E.; Berghmans, H. *J. Mol. Struct.* **2000**, *554*, 55.
(65) Burchard, W. *Light Scattering Principles and Development*; Clarendon Press: Oxford, 1996.

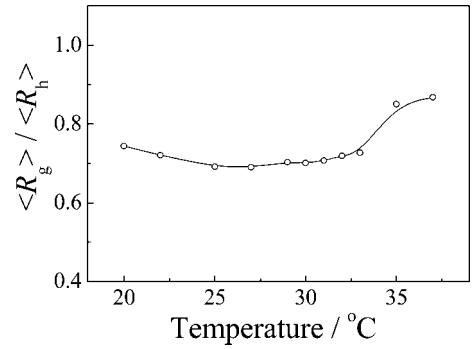

Figure 8. Temperature dependence of $\langle R_g \rangle / \langle R_h \rangle$ ratios obtained for 5×10^{-6} g/mL aqueous solution of hybrid silica nanoparticles coated with PNIPAM brushes.

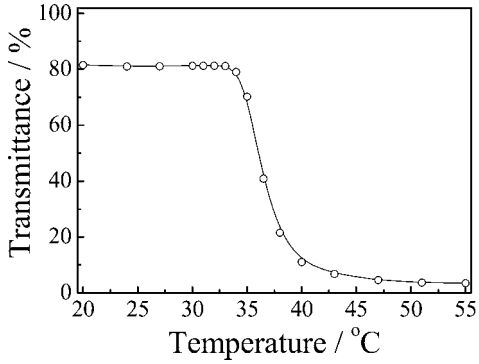

Figure 9. Temperature-dependent optical transmittance at 800 nm obtained for 5.0×10^{-4} g/mL aqueous solution of hybrid silica nanoparticles coated with PNIPAM brushes.

For uniform nondraining spheres, hyperbranched clusters, and random coils, $\langle R_g \rangle / \langle R_h \rangle$ ratios are predicted to be ~0.774, 1.0–1.2, and 1.5–1.8, respectively.[65] We also plotted the temperature dependence of $\langle R_g \rangle / \langle R_h \rangle$ ratios which can reflect the conformation of polymer chains or particles (Figure 8). At 20 °C, $\langle R_g \rangle / \langle R_h \rangle$ of hybrid silica nanoparticles is ~0.74, which is less than that of a uniform hard sphere. This can be attributed to higher chain density of the inner layer compared to the outer zone. $\langle R_g \rangle / \langle R_h \rangle$ decreases from 0.74 to 0.69 in the temperature range of 20–27 °C. Above 30 °C, $\langle R_g \rangle / \langle R_h \rangle$ gradually increases and finally stabilizes out at higher temperatures.

In comparison with a uniform hard sphere with the same size, the denser core leads to a smaller $\langle R_g \rangle$, but the same $\langle R_h \rangle$, so that the decrease of $\langle R_g \rangle / \langle R_h \rangle$ in the range 20–27 °C corresponds to the temperature range where the inner part of PNIPAM brushes starts to collapse. The increase of $\langle R_g \rangle / \langle R_h \rangle$ above 30 °C should be due to extensive collapse of PNIPAM brushes including the outer zone, which can concomitantly decrease $\langle R_g \rangle$ and $\langle R_h \rangle$. Theoretically, the collapse of the outer region will lead to more prominent decrease of $\langle R_h \rangle$ compared to that of $\langle R_g \rangle$.

Turbidity Measurements. Figure 9 shows the temperature dependence of optical transmittance at 800 nm obtained for the aqueous solution of PNIPAM grafted hybrid silica nanoparticles. A much higher concentration (5.0×10^{-4} g/mL) compared to that for LLS studies was employed to have enough detection sensitivity. The optical transmittance exhibits no changes in the range of 20–33 °C, where LLS results already reveal the collapse of the inner part of PNIPAM brushes (Figure 7). In this temperature range, the outer zone of PNIPAM brushes still remains well-solvated and aggregation between particles does not occur.

Above 33 °C, transmittance decreases abruptly from 80% to ~5% in the temperature range 33–47 °C due to the aggregation of hybrid nanoparticles. Hybrid nanoparticles with already collapsed PNIPAM brushes tend to collide with each other at such high concentrations. This type of collision will surely contribute to the aggregation between different hybrid nanoparticles since the PNIPAM corona becomes "sticky" above the critical phase transition temperature.

Conclusion

Narrow-disperse thermoresponsive hybrid silica nanoparticles densely grafted with PNIPAM brushes (2.2 nm^2/chain determined by TGA and 1.85 nm^2/chain by LLS) were synthesized by surface-initiated ATRP of NIPAM from 2-bromoisobutyrate-functionalized silica nanoparticles. The polymerization was conducted in a controlled manner, as revealed by the linear kinetic plot, linear increase of molecular weights (M_n) with monomer conversions, and narrow molecular weight distributions of grafted PNIPAM chains. LLS characterization of hybrid nanoparticles revealed that surface grafted PNIPAM brushes exhibit two-stage collapse upon heating, supporting double phase transitions observed by Tenhu et al.[40] and Liu et al.[61,62] for different systems. As the current system was based on well-defined hybrid silica nanoparticles coated with PNIPAM brushes of controlled thickness, the M_n of grafted PNIPAM chains was relatively high (18 400 Da) and the end group (–Cl or –Br) hydrophobicity was negligible; we tentatively expect that the double phase transition behavior is characteristic of polymer brushes densely and covalently grafted at the surface of spherical nanoparticles. This unique property of polymer brushes can be further utilized to fabricate novel nanostructured devices with more complex functions.

Acknowledgment. This work was financially supported by an Outstanding Youth Fund (50425310) and research grants (20534020 and 20674079) from the National Natural Scientific Foundation of China (NNSFC), the "Bai Ren" Project and Special Grant (KJCX2-SW-H14) of the Chinese Academy of Sciences, and the Program for Changjiang Scholars and Innovative Research Team in University (PCSIRT).

Supporting Information Available: Micro-DSC characterization of PNIPAM chains cleaved from hybrid silica nanoparticles. This information is available free of charge via the Internet at http://pubs.acs.org.

CM702073F